



Research paper

Removal of bisphenol A and trichlorophenol from aqueous solutions by adsorption with organically modified bentonite, activated carbon composites: A comparative study in single and binary systems

Kamel Noufel^{a,*}, Nassima Djebri^b, Nadia Boukhalfa^c, Mokhtar Boutahala^c, Achour Dakhouché^a

^a Laboratoire des Matériaux Inorganique (LMI), Faculté des Sciences, Université Mohamed Boudiaf, 28000, M'Sila, Algeria

^b Université de Bordj Bou Arreridj, El Annasser, 34000, BBA, Algeria

^c Laboratoire de Génie des Procédés Chimiques (LGPC), Faculté de Technologie, Université Ferhat Abbas Sétif-1-19000, Sétif, Algeria

ARTICLE INFO

Keywords:

Adsorption
Organo-activated-bentonite
Activated carbon
Alginate
Composite
Competition
Emerging pollutant

ABSTRACT

Three adsorbents have been developed by encapsulation of organo-activated bentonite (OAB), activated carbon (AC) and organo-activated bentonite/activated carbon (AC-OAB) in cross-linked alginate beads (A) with the aim of using them in the removal of bisphenol A (BPA) and 2,4,5-trichlorophenol (TCP). The adsorption capacities of the three adsorbents were investigated in order to choose the best adsorbent for BPA and TCP. The alginate/activated carbon beads (A-AC) exhibit the maximum BPA and TCP adsorption capacities (419.3 and 444.7 mg/g at 25 °C, respectively). In the binary system, a decrease was observed at the adsorbed amount to 291.5 mg/g for BPA and 430.2 mg/g for TCP. The adsorption of BPA and TCP by A-AC composite beads was studied and the effects of solution pH value, temperature and contact time on the adsorption were investigated. Results revealed that BPA and TCP adsorption kinetics onto A-AC are best described by the pseudo-second order model, and the equilibrium adsorption data are well fitted to both Langmuir and Freundlich models. The zero point charge determination (pH_{PZC}), the scanning electron microscopy (SEM) and Fourier transform infrared spectroscopy (FTIR) analysis were carried out. The A-AC composite was used for six cycles without significant adsorptive performance loss. Therefore, the ecofriendly prepared A-AC adsorbent was considered as highly recyclable and efficient adsorbent for BPA and TCP pollutants.

1. Introduction

The increase in the consumption of living standards such as personal and household care products, pesticides, pharmaceuticals etc, amplify the pollution of water and make the world experienced the adverse consequences of uncontrolled human activities (Deblonde et al., 2011; Pham and Proulx, 1997; Rosal et al., 2010). The pollution of water present a big environmental issue, therefore, the removal of emerging contaminants from wastewater is very important.

Changes in the conventional approach to pollution, prevention and control are required now due to the particular characteristics of contaminant products (Vogelsang et al., 2006; Achak et al., 2009). For the removal of emerging contaminants from water as well as wastewater, advanced oxidation processes, nanofiltration, and reverse osmosis membranes are used as treatment options (Bolong et al., 2009; Rossner et al., 2009). However, the high investment, the maintenance

costs, the secondary pollution and the complicated procedure involved in these treatment processes are considered as the shortcomings of most of them. On the other hand, physicochemical treatments such as coagulation/flocculation processes were generally unable to remove many kinds of contaminants such as endocrine disrupting compounds (EDCs) (Rossner et al., 2009; Suarez et al., 2009).

Conversely, adsorption processes have been found to be superior to other techniques for wastewater treatment in terms of do not add undesirable by-products, simplicity of operation, and insensitivity of toxic compounds (Tong et al., 2010). Among several used adsorbents, commercial activated Carbons (ACs) have been used for the removal of different types of emerging pollutants, but their use is limited due to the high cost. This make various workers try to prepare low cost alternative adsorbents, which may replace activated carbons used in pollution control through adsorption process (Gupta et al., 2009; Boukhalfa et al., 2016). Recently, natural residue materials that are available in large

* Corresponding author.

E-mail address: kamel.noufel@univ-msila.dz (K. Noufel).

<https://doi.org/10.1016/j.gsd.2020.100477>

Received 16 March 2020; Received in revised form 23 August 2020; Accepted 26 August 2020

Available online 31 August 2020

2352-801X/© 2020 Elsevier B.V. All rights reserved.

quantities from nature have been used as low cost adsorbents (Boukhalfa et al., 2016; Djebri et al., 2016, 2017). Moreover, the use of these materials directly or after some treatments is becoming vital concern because they represent unused resources, which causes disposal problems (Gholizadeh et al., 2013; Zhou et al., 2016; Chang et al., 2012).

Clay minerals are argillaceous materials that have been widely used to remove toxic, metal ions, dyes, chlorophenols and drugs. Due to their high specific surface area, high cation exchange capacity (CEC), chemical and physical stability, abundance and inexpensiveness, they can be effectively employed as adsorbents for many waste water pollutants (Gupta et al., 2009; Boukhalfa et al., 2016; Djebri et al., 2017). To improve adsorption of organic pollutants, many researchers have focused on the surface modifications of clay by: (1) the treatment of clay minerals with concentrated inorganic acids usually HCl or H₂SO₄ at high temperature and (2) exchanging interlayer inorganic cations (e.g., H⁺, Na⁺, K⁺, Ca²⁺) with organic cations such as quaternary alkylammonium (Djebri et al., 2016; Gholizadeh et al., 2013). It was known that the modification of clay with inorganic acid increases the surface specific area, porosity, surface acidity and improve the adsorption properties of the clay by increasing the number of active sites. In addition, the treatment of clay by the surfactant molecules changes the properties of the clay from hydrophilic to hydrophobic, and organophilic. It also increases the basal spacing of the layers. Thus, organophilic clay can have various applications, especially as adsorbents for a great variety of organic pollutants. Thus, both these clay minerals and activated carbon lose a substantial amount of their adsorption capacity when they are regenerated for reuse.

In the present work, alternative composite materials resulting from the combination of modified bentonite clay and/or synthesized activated carbon were prepared by encapsulation in cross-linked alginate beads. These composite materials may offer combined properties (thermal, mechanical and porosity properties) compared with the characteristics of the bare individual activated carbon, bentonite and alginate polymer (Djebri et al., 2016; Hassan et al., 2014a, 2014b; Luo et al., 2020; Belhouchat et al., 2017). Their adsorption characteristics were assessed by using bisphenol A (BPA) and 2,4,5 trichlorophenol (TCP) as adsorbate. The effect of the initial concentration, pH, temperature and contact time on adsorption was monitored and optimal experimental conditions were determined. Different adsorption isotherms (Langmuir and Freundlich isotherms) and kinetic models (pseudo-first, second-order kinetics, intraparticle and film diffusion) were used to find out the most suitable models describing our experimental findings. The best adsorbent loaded with BPA and TCP is regenerated by elution method and the competitive adsorption of BPA and TCP was also studied.

2. Materials and methods

2.1. Materials

Apricot stone was obtained locally (region Setif-Algeria). Raw bentonite (RB) was obtained from HammamBouhrara in Maghnia (West Algeria). The chemical composition of the RB was reported in our

earlier publication (Djebri et al., 2017). Alginate (A), cetyltrimethylammonium bromide (CTAB) (C₁₉H₄₂NBr, > 98%), bisphenol A (BPA), 2,4,5-trichlorophenol (TCP), sodium chloride (NaCl), sulfuric acid (H₂SO₄) were all purchased from Sigma-Aldrich (USA). The physicochemical properties of phenolic compounds are given in Table 1. Distilled water was used in all experiments.

2.2. Preparation of adsorbents materials

Organo-activated bentonite (OAB) was prepared as described previously. Briefly, organo-acid-activated bentonite (OAB) was prepared in two steps. In the first step, the purified bentonite was subjected to acid treatment with sulfuric acid H₂SO₄ 1 M (1:1 w/w) with stirring and reflux heating as described previously. In the second step, AB (activated bentonite) was treated with cetyltrimethylammonium bromide (CTAB) as described in details previously in (Djebri et al., 2017). The resulting material was named as organo-activated bentonite (OAB).

Activated carbon (AC) was prepared by chemical activation using phosphoric acid according to the method of Y. Sun et al. (2012). Briefly, chemical impregnation was carried out in a round-bottom flask reactor, where 20 g of precursor (Apricot Stone) reacted with a 40 wt % H₃PO₄ solution at a ratio of 1:2 (AS/H₃PO₄) under stirring for 6 h, and then, the mixture were filtered under vacuum to remove the excess of phosphoric acid, then the solid was calcined at 450 °C for 1 h, defining a heating ramp of 10 °C/min. The resulting carbon was washed with distilled water in order to remove the remaining phosphoric acid until the solution pH reaches 6.5. Finally, the solid was dried in oven at 110 °C for 24 h. The resulting material was named as activated carbon (AC).

Composite materials: A solution of 1% sodium alginate was prepared in deionized water in a 250 mL flask under stirring for 2 h. Same amount (2 g) of organo-activated bentonite (OAB) or/and activated carbon (AC) was added. The mixture was stirred for 24 h at room temperature (25 °C). The homogenous mixture was dropped into a flask containing CaCl₂ (4%, w/v) solution to produce calcium alginate/organo activated bentonite (A-OAB), calcium alginate/activated carbon (A-AC) and calcium alginate/organo-activated bentonite/activated carbon (A-AC-OAB) composite beads. The collected material beads were washed, dried and stored separately in a clean dry glass bottles for subsequent use.

2.3. Batch adsorption

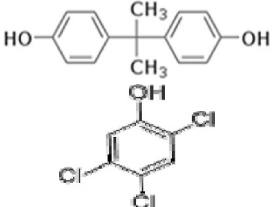
The adsorption of BPA and TCP was conducted in a static batch experiment. An aqueous solution of certain concentration of adsorbate (20–500 mg/L) was shaken in bottles of 200 mL capacity with 1 g/L of adsorbents A-OAB, A-AC and A-AC-OAB for 96 h. The supernatant liquid was separated out, where the equilibrium concentration of the BPA and TCP was determined using Shimadzu UV-1700 spectrophotometer (at 276 and 290 nm, respectively).

The adsorbed amount at equilibrium, q_e (mg/L) was calculated by:

$$q_e = \frac{(C_0 - C_e) \cdot V}{m} \quad (1)$$

The percentage removal (R %) by the adsorbent was expressed by:

Table 1
Physicochemical properties of TCP and BPA.

Compound	MW(g/mol)	Water solubility (mg/L), at 25 °C	Dissociation constant (pKa)	Log K _{ow}	Chemical structure
BPA (C ₁₅ H ₁₆ O ₂)	228.29	120–300	9.6–10.2	3.32	
TCP (C ₆ H ₃ Cl ₃ O)	197.45	1200	6.7–6.94	3.66	

$$R(\%) = \frac{(C_0 - C_e) \cdot 100}{C_0} \quad (2)$$

where C_0 and C_e (mg/L) are the liquid – phase concentration of BPA or TCP at initial time and equilibrium, respectively, V is the volume of the solution (L) and m is the weight (g) of the adsorbent.

2.4. Kinetic study

Time dependence adsorption of BPA and TCP was carried out from 0 h to 96 h using 0.2 g of adsorbent with 200 mL of adsorbate solution at a constant temperature (25 °C) with a concentration from 30 to 300 for BPA and from 15 to 400 mg/L for TCP, respectively. The concentration of adsorbate after recorded time intervals is determined. The adsorption capacity q_t (mg/L) at different contact time t (h) was determined using the following equation:

$$q_t = \frac{(C_0 - C_t) \cdot V}{m} \quad (3)$$

where C_t (mg/L) is the concentration of BPA or TCP at time t (h) in the solution.

2.5. Binary adsorption studies

The first step was to examine the adsorption of BPA at equilibrium (concentration of BPA ranging from 20 to 300 mg/L) in the presence of TCP (50 mg/L). For the next step, a series of binary solutions where the concentration of BPA was fixed at 50 mg/L, and the concentration of TCP was varied from 20 to 400 mg/L were prepared. These binary solutions were stirred at 200 rpm for 96 h at 25 ± 1 °C, and solution pH 7.0 for the first step and pH 4.0 for the second step. A correction was applied for the spectrophotometric determination of residual concentrations in mixture systems by using equations (4) and (5):

$$C_{BPA} = \frac{k_{TCP2} d_{\lambda 1} - k_{TCP1} d_{\lambda 2}}{k_{BPA1} k_{TCP2} - k_{BPA2} k_{TCP1}} \quad (4)$$

$$C_{TCP} = \frac{k_{BPA1} d_{\lambda 2} - k_{BPA2} d_{\lambda 1}}{k_{BPA1} k_{TCP2} - k_{BPA2} k_{TCP1}} \quad (5)$$

where C_{BPA} , C_{TCP} , k_{BPA1} , k_{BPA2} , k_{TCP1} , k_{TCP2} , $d_{\lambda 1}$, and $d_{\lambda 2}$ are the concentration of BPA and TCP, the calibration constants for BPA and TCP at their characteristic adsorption wavelength (i.e., k_1 and k_2), and the optical densities at the two wavelengths λ_1 and λ_2 , respectively.

2.6. Desorption and regeneration of A-AC

Desorption study was conducted using ethanol as desorption eluent. Adsorption was first conducted using the optimal procedure in section 2.3. Then the A-AC with adsorbed BPA or TCP was separated from the solutions. Subsequently, the supernatant solutions were discarded and the A-AC adsorbent was washed with distilled water. Finally, the BPA or TCP were desorbed from the A-AC with 50 mL of ethanol. To investigate the regeneration of the adsorbent, A-AC was reused after desorption in adsorption experiments and the process was repeated six times. The percentage of desorption of BPA or TCP was calculated by the following equation:

$$R\% = \frac{m_{des}}{m_{ads}} \times 100 \quad (6)$$

where m_{des} (mg) and m_{ads} (mg) are the amounts of desorbed and adsorbed BPA or TCP, respectively.

2.7. Error analysis

The values of the kinetic and isotherm parameters were determined

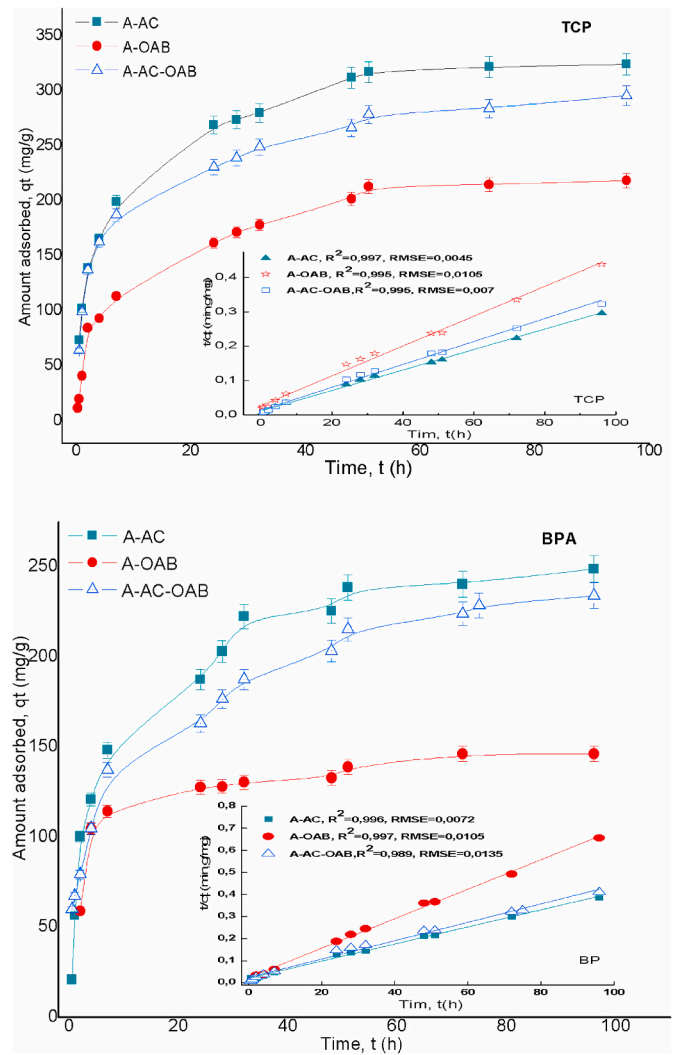


Fig. 1. Effect of contact time on BPA and TCP adsorption onto A-AC, A-OAB and A-AC-OAB composites ($C_0 = 300$ mg/L, $T \sim 25$ °C, $C_{ads} = 1$ g/L).

by the regression analysis using ORIGIN program (version 8). The correlation coefficient (R^2) and residual root-mean squared error (RMSE) were used to analyse the data set and to confirm the best fit kinetics and isotherm model for the adsorption. If data from the model are similar to those obtained in experiments, R^2 will be close to 1 and RMSE will be a low value. The R^2 and RMSE were evaluated using Eqs. (7) and (8).

$$R^2 = 1 - \frac{\sum_{n=1}^n (q_{e,t,exp,n} - q_{e,t,cal,n})^2}{\sum_{n=1}^n (q_{e,t,exp,n} - \overline{q_{e,t,exp,n}})^2} \quad (7)$$

$$RMSE = \sqrt{\frac{1}{n-1} \sum_{n=1}^n (q_{e,t,exp,n} - q_{e,t,cal,n})^2} \quad (8)$$

where $q_{e,t,exp}$ and $q_{e,t,cal}$ are the experimental adsorption capacity at equilibrium ($q_{e,exp}$) or at any time ($q_{t,exp}$) and the calculated adsorption capacity at equilibrium $q_{e,cal}$ or at any time $q_{t,cal}$ from the models, respectively.

2.8. Characterization of adsorbents

The morphological structure of the investigated samples was examined by scanning electron microscopy (SEM) using SEM model (JSM-

Table 2

Kinetic parameters for the adsorption of TCP and BPA onto A-AC, A-AC-OAB and A-OAB composites.

(TCP)	Models	Parameters	A-AC	A-OAB	A-AC-OAB
	Pseudo first-order model	$K_1 \times 10^{-2}$	3.6	3.3	3.9
	$\ln(q_e - q_t) = \ln q_e - k_1 \times t$	$\ln q_{cal}$	5.23085	5.09133	5.21843
		R^2	0.921	0.929	0.975
		RMSE	0.321	0.282	0.196
	Pseudo second-order model	$K_2 \times 10^{-4}$	7.6	7.04	8.14
	$(t/q_t) = (1/k_2 q_e^2) + (t/q_e)$	q_{cal}	335.6	229.9	299.4
		R^2	0.997	0.995	0.995
		RMSE	0.0045	0.0105	0.007
	Intraparticle diffusion model	K_3	28.2	23.0	23.7
	$q_t = k_3 \sqrt{t} + C$ Whole time	R^2	0.891	0.906	0.890
		RMSE	30.10	23.32	25.44
	Film diffusion model	K_4	0.0355	0.033	0.039
	$-\ln(1 - q_t/q_e) = k_4 t$	R^2	0.921	0.929	0.975
		RMSE	0.3215	0.2819	0.1965
		q_{exp}	280	220	250
(BPA)		Parameters	A-AC	A-OAB	A-AC-OAB
	Pseudo first-order model	$K_1 \times 10^{-2}$	3.25	3.14	3.37
	$\ln(q_e - q_t) = \ln q_e - k_1 \times t$	$\ln q_{cal}$	5.1	4.0	5.1
		R^2	0.927	0.903	0.988
		RMSE	0.281	0.314	0.117
	Pseudo second-order model	$K_2 \times 10^{-4}$	7.20	19.0	7.2
	$(t/q_t) = (1/k_2 q_e^2) + (t/q_e)$	q_{cal}	258.4	149.9	240.4
		R^2	0.996	0.997	0.990
		RMSE	0.007	0.010	0.013
	Intraparticle diffusion model	K_3	23.5	7.99	19.81
	$q_t = k_3 \sqrt{t} + C$ Whole time	R^2	0.862	0.704	0.953
		RMSE	28.74	14.1	13.9
	Film diffusion model	K_4	0.0032	0.0031	0.0034
	$-\ln(1 - q_t/q_e) = k_4 t$	R^2	0.927	0.902	0.988
		RMSE	0.281	0.314	0.117
		q_{exp}	250	147	235

6830 L V, JEOL).

Fourier transform infrared spectroscopy (FTIR) analysis of the adsorbent before and after adsorption was carried out in KBr pellets in the range of 4000–400 cm^{-1} with 4 cm^{-1} resolution using PerkinElmer spectrum FT-IR model 65 spectrometer.

The pH_{PZC} (point of zero charge) values of (A, AC and A-AC) were obtained using the same method in previous paper (Djebri et al., 2016). In brief, the initial pH (pH_i) of 0.01 M NaCl solutions (50 mL) were adjusted to a pH range of 2–10 using 0.1 and 0.01 M HCl or NaOH. Then, 0.2 g of adsorbent was added to each sample. The dispersions were stirred for 48 h at 25 °C, and the final pH of the solutions (pH_f) was determined. The point of zero charge was obtained from a plot of ($\text{pH}_f - \text{pH}_i$) versus pH_i .

3. Results and discussion

3.1. Adsorption kinetic

The adsorption kinetics of BPA and TCP performed with three adsorbents (A-OAB, A-AC and A-AC-OAB) are plotted on Fig. 1. The adsorption kinetic study was done at the same concentration of 300 mg/L onto the three composites. The adsorption uptake of BPA and TCP increases gradually with increasing in contact time. Fig. 1, show that, equilibrium time required for adsorption is not less than 50 h. The adsorbed amounts of BPA and TCP at equilibrium are (147, 220 mg/g), (235, 250 mg/g) and (250, 280 mg/g), for A-OAB, A-AC-OAB and A-AC, respectively. The experimental and calculated parameters of the pseudo-first-order and the pseudo-second-order equations are listed in Table 2. It can be seen that the R^2 and RMSE values for the pseudo-first-order model did not show a consistent trend and the experimental q_e ($q_{e,\text{exp}}$) values did not well agree with the calculated values ($q_{e,\text{cal}}$) obtained from the linear plots (Figure not shown). This shows that adsorption of the two emerging pollutants onto all adsorbents does not follow a pseudo first-order kinetic model. However, all the R^2 and the RMSE values

obtained from the pseudo-second-order model are close to one with a good agreement between the experimental q_e values and the calculated values obtained from the linear plots (Fig. 1 insets). These results indicate that the pseudo-second-order model describes better the experimental data. According to previous studies the pseudo-second-order model assumes that the rate-limiting step is the chemical binding process involving sharing or exchange of electrons between adsorbent and adsorbate (El Fargani et al., 2017).

The experimental data were also tested by the intraparticle and film diffusion models. According to intraparticle diffusion, Weber and Morris equation (See Table 2), if the plot of q_t vs. $t^{1/2}$ gives a straight line and the plot passes through the origin, the adsorption process is controlled by intraparticle diffusion only. If the data exhibit multi-linear plots, then two or more steps influence the adsorption process (El Fargani et al., 2017). In Fig. 2, the linear lines of the second and third stages did not pass through the origin and this deviation from the origin or near saturation might be due to the difference in the mass transfer rate in the initial and final stages of adsorption (Belhouchat et al., 2017). It shows that intraparticle diffusion was not the only rate limiting mechanism in the adsorption process, but another process may also be involved in the adsorption process. The values of k_{pi} , C_i and correlation coefficient, R^2 and RMSE obtained for the plots are given in Table 2. The k_{pi} values were found to be generally increased with the increasing in BPA or TCP initial concentrations, which is due to the greater driving force (Sdiri et al., 2014). The adsorption process follows the film mechanism when the plots of $\ln(1 - q_t/q_e)$ versus t at different initial concentrations are linear or non-linear but does not pass through the origin. The Boyd plots are linear (Fig. 2 insets) but do not pass through the origin, thereby explaining the influence of film diffusion mechanism on the adsorption rate. Likewise, by comparing the data presented in Table 2, the R^2 and RMSE values for the film diffusion model were higher than those of intraparticle diffusion model, thereby suggesting that film diffusion controls the adsorption rate of BPA and TCP onto all samples under the studied conditions.

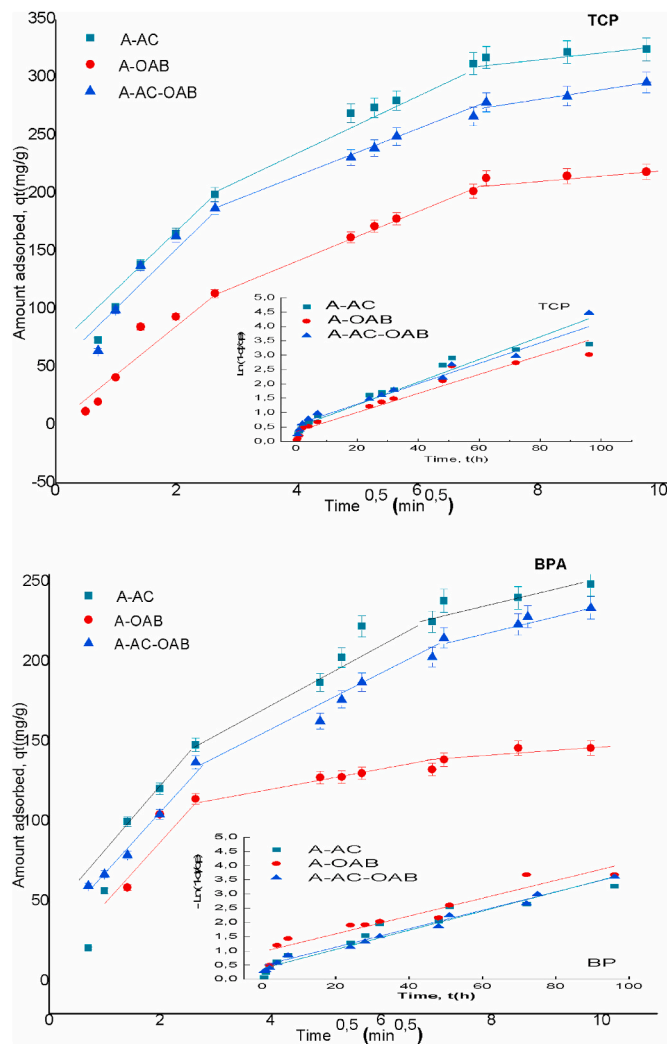


Fig. 2. Plot of intraparticle and film diffusion model for adsorption of BPA and TCP onto A-AC, A-OAB and A-AC-OAB composites.

3.2. Adsorption isotherm

Adsorption isotherm studies were done to predict the interactions between the adsorbate molecules and the surface of the adsorbent material. In this part, the adsorption isotherms of BPA and TCP were studied onto A-OAB, A-AC and A-AC-OAB in single system and onto A-CA in binary system.

3.2.1. Single system of BPA and TCP onto A-OAB, A-AC and A-AC-OAB

The adsorption isotherms of BPA and TCP onto A-OAB, A-AC and A-AC-OAB were demonstrated in Fig. 3. The shape of the isotherm provides information about the adsorption mechanisms. According to Giles classification (Mavinkattimath and Kodialbail, 2017), the BPA and TCP adsorption onto samples forms an L-shape curve, which indicates that these molecules are probably adsorbed in a flat position because of the low competition from solvent molecules. To understand the adsorption mechanism, the data are simulated by Langmuir and Freundlich isotherm models by the following equations, respectively:

$$q_e = \frac{q_m K_L C_e}{1 + K_L C_e} \quad (9)$$

$$q_e = K_F C_e^{1/n_F} \quad (10)$$

where q_m is the maximum adsorption capacity, K_L is the Langmuir

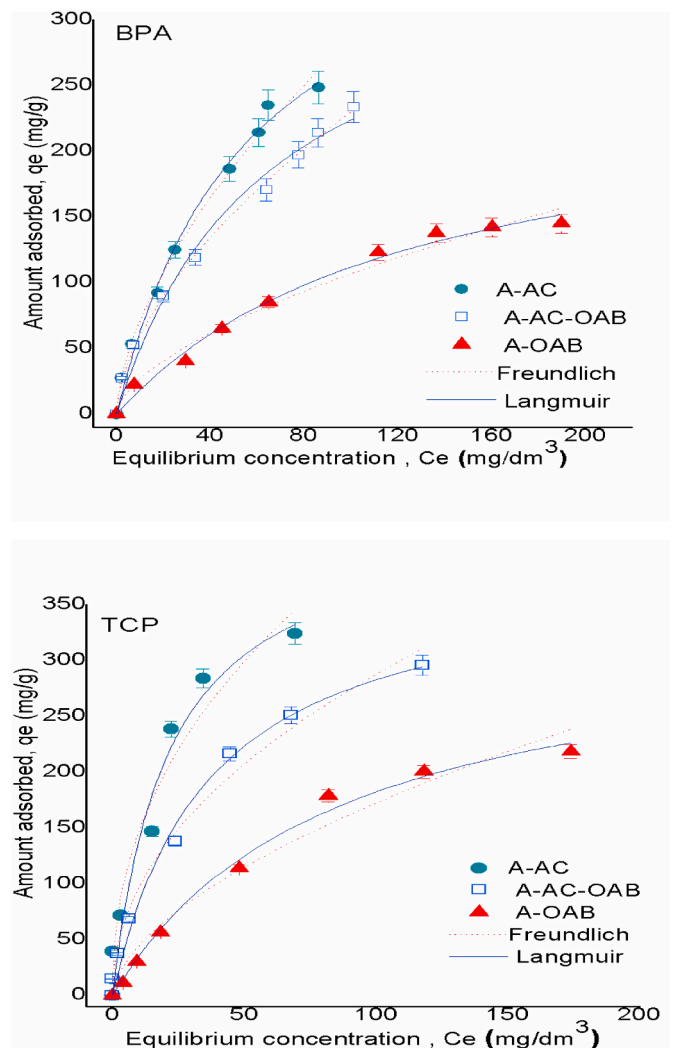


Fig. 3. Equilibrium adsorption isotherms of BPA and TCP onto A-AC, A-OAB and A-AC-OAB at 25 °C fitted to Langmuir and Freundlich models.

Table 3

Langmuir, Freundlich isotherm parameters for the adsorption of TCP and BPA onto A-AC, A-AC-OAB and A-OAB composites.

Adsorbate	Model	Parameter	Samples		
TCP	Langmuir	q_m	A-AC	A-AC-OAB	A-OAB
		$K_L \cdot 10^{-2}$	444.73	385.08	336.72
		R^2	4.46	2.76	1.18
		R^2	0.971	0.988	0.992
		RMSE	22.30	8.40	13.32
	Freundlich	K_F	51.39	32.59	11.59
		n	2.208	2.119	1.706
		R^2	0.962	0.954	0.966
		RMSE	25.62	17.8	15.4
BPA	Langmuir	q_m	A-AC	A-AC-OAB	A-OAB
		$K_L \cdot 10^{-2}$	419.33	368.22	252.89
		R^2	1.75	1.55	0.79
		R^2	0.991	0.984	0.989
		RMSE	9.76	10.50	5.78
	Freundlich	K_F	19.15	15.45	6.74
		n	1.656	1.706	1.669
		R^2	0.992	0.998	0.979
		RMSE	13.12	3.30	7.89

constant, K_F and n_F are the Freundlich constants. The R^2 values and RMSE shown in Table 3, indicate that the adsorption data are well fitted to both Langmuir and Freundlich models. There is a possibility of mono

and heterolayer compounds formation on the adsorbent surface. This observation is similar to reported findings (Achak et al., 2009). As shown in Table 3, the predicted maximum adsorption capacity of BPA and TCP on A-AC, A-AC-OAB and A-OAB at 298 K is 419.3, 368.3, 252.9 mg/g and 444.8, 385.0, 336.7 mg/g, respectively. Adsorption intensity parameters n from Freundlich model were ranged between 1.0 and 10 confirming the favorable adsorption process. Thus, A-AC is a very efficient adsorbent for the removal of BPA and TCP from wastewater. Based on the preliminary assessment of the different composites in terms of the percentage removal of BPA and TCP, A-AC was the best adsorbent among the samples tested. Therefore, all further experiments were performed using the A-AC composite.

3.2.2. Binary system of BPA and TCP onto A-AC

To study the involved interactions during the adsorption process, a single adsorbate is normally chosen. However, pollutants are regularly manifold and complex in wastewaters. Nevertheless, studies of multi-component systems are less frequent even if they are closely related to improve the efficiency of water treatment. Therefore, the competitive adsorption of emerging compounds in the mixtures of BPA/TCP onto A-AC was investigated by studying the effect of the presence of one of them (its constant initial concentration is 50 mg.L⁻¹) on the adsorption of the second one (at different concentrations). The effect of competitive adsorption of BPA and TCP onto A-AC were shown in Fig. 4. The isotherm data of the binary solution systems were analyzed using the Langmuir (Eq. (9)), Freundlich (Eq. (10)) and extended Langmuir

Table 4

Langmuir, Freundlich and extended Langmuir isotherm parameters for the adsorption of TCP and BPA onto A-AC composite in single and binary system.

		BPA	BPA+50 mg/ L TCP	TCP	TCP+50 mg/ L BPA
Langmuir	q_m	419.33	291.48	444.73	430.16
	$K_L \cdot 10^{-2}$	1.75	2.46	4.46	2.3
	R^2	0.991	0.989	0.971	0.994
	RMSE	9.76	8.26	22.30	8.18
Freundlich	K_F	19.15	17.97	51.39	23.72
	N	1.656	1.838	2.208	1.764
	R^2	0.992	0.986	0.962	0.984
	RMSE	13.12	9.45	25.62	13.16
Extended Langmuir	$q_{m,i}$		257.1		392.2
	K_L		3.6		2.9
	$i \cdot 10^{-2}$				
	R^2		0.965		0.956

models (Eqs. (11) and (12)).

The extended Langmuir model can be expressed as (Zhou et al., 2012):

$$q_{e,1} = \frac{q_{m,1} * K_{L,1} * C_{e,1}}{1 + K_{L,1} C_{e,1} + K_{L,2} C_{e,2}} \quad (11)$$

$$q_{e,2} = \frac{q_{m,2} * K_{L,2} * C_{e,2}}{1 + K_{L,1} C_{e,1} + K_{L,2} C_{e,2}} \quad (12)$$

where $K_{L,1}$, $K_{L,2}$, $q_{m,1}$ and $q_{m,2}$ are the Langmuir isotherm model parameters obtained from Eq. (9) in the single solute system. From equations (11) and (12), we have equation (13):

$$K_{L,2} C_{e,2} / K_{L,1} C_{e,1} = q_{m,1} q_{e,2} / q_{m,2} q_{e,1} \quad (13)$$

The linear form of extended Langmuir isotherm in binary system was obtained following Eq. (14) (El Fargani et al., 2017).

$$C_{e,1} / q_{e,1} = 1 / K_{L,1} q_{m,1} + C_{e,1} / q_{m,1} + q_{e,2} C_{e,1} / q_{e,1} q_{m,2} \quad (14)$$

According to Eq. (14), the values of $C_{e,1} / q_{e,1}$ had linear correlation with $C_{e,1}$ and $q_{e,2} C_{e,1} / q_{e,1} q_{m,2}$ if the adsorption describe the extended Langmuir model. According to the trend in Fig. 4 and the high values for R^2 (Table 4), the adsorption of BPA and TCP from binary molecule solutions was best described by the Langmuir isotherm model, indicating the adsorbates molecules were adsorbed at well-defined sites and there were no interactions between molecules adsorbed on adjacent sites. These results showed that the binary system adsorption onto A-AC is monolayer and homogeneous in nature. Compared to those of the single emerging compound system, the q_{max} values of the two compounds decreased in binary systems. For example, the q_{max} of TCP and BPA decreased from 444.7 to 430.2 mg/g and from 419.6 to 291.5 mg/g, respectively. This means that the adsorption of TCP or BPA onto A-AC was affected by the presence of BPA or TCP, respectively. In addition, the values of q_e^b (binary solution system) / q_e^s (single solution system) for both BPA (0.6949 when the addition of 50 mg/L of TCP) and TCP (0.9673 when the addition of 50 mg/L of BPA) were found to be less than 1.0, suggesting that simultaneous presence of both phenolic compound molecules reduced the adsorption through competition for binding sites on the A-AC. The results indicate that there is competition between the EDCs for the adsorption sites on A-AC (Ahmaruzzaman and Reza, 2015). The results confirm also that the preferential adsorption by A-AC was given to TCP. This difference in behavior is probably attributed to the different octanol-water partitioning coefficients ($\log K_{ow}$) of each compound, which results in different hydrophobic interaction densities with A-AC adsorbent. Indeed, TCP is more hydrophobic ($K_{ow} = 3.66$) than BPA (3.32). This difference determines the extent of the adsorption affinity, resulting in the preferential adsorption of A-AC for TCP. Similar results have been reported by previous works (Djebri et al., 2017).

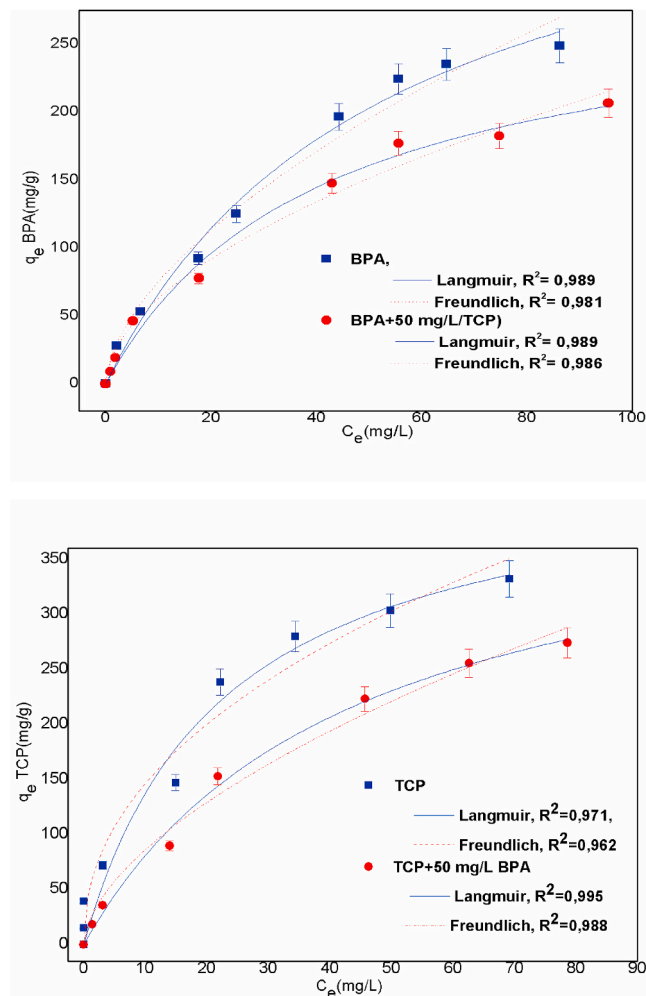


Fig. 4. Freundlich and Langmuir isotherm model of BPA (a) and TCP (b) adsorption onto A-AC in single and binary system.

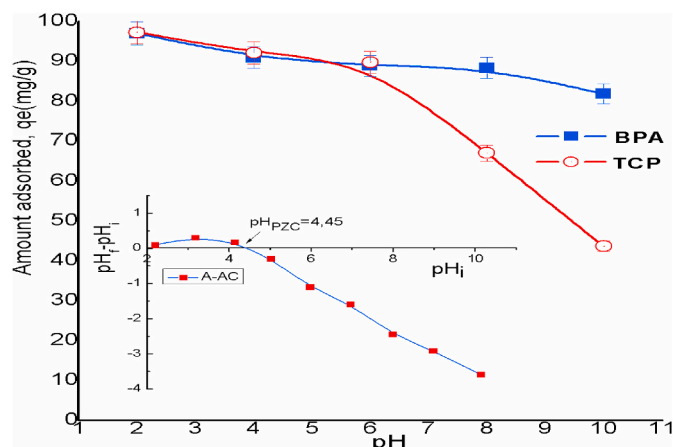


Fig. 5. Effect of solution pH on BPA and TCP removal at 25 °C (BPA or TCP initial concentration = 100 mg/L).

3.3. Effect of pH on BPA/TCP removal by A-AC

The effect of solution pH on the adsorption onto A-AC was examined from pH 2 to 10. The adsorbate initial concentration (100 mg/L) with solid dose (1 g/L) is taken as constant at constant temperature of 25 °C and the pH was adjusted using 0.1 and 1.0 M HCl or NaOH.

The removal percentage of BPA and TCP by A-AC at different pH values is plotted in Fig. 5. As can be seen from this plot, the BPA and TCP removal was found to decrease significantly with increase in initial solution pH from 2 to 10. In this study, the highest BPA and TCP removal was achieved at pH 2, with a maximum removal of 97.8%. Similar results have been reported for the adsorption of 2,4-DCP and 2,4,6-TCP by oil palm empty fruit bunch-based activated carbon (Tan et al., 2009; Shaarani and Hameed, 2010), palm pith carbon (Sathishkumar et al., 2007) and Cattail fiber (Ren et al., 2011). BPA and TCP are weakly acidic compounds that ionize at a certain pH. The pH_{PZC} for A-AC was 4.43. The surface charge of A-CA below pH 4.43 ($pH < pH_{PZC}$) is positive and in more acidic medium ($pH < pK_a$ 6.8 and 9.6 for BPA and TCP, respectively), the phenolic compounds are in the non-dissociated forms. In this case, the dispersion interactions predominate in the adsorption process. However, at basic pH ($pH > pK_a$), the BPA and TCP dissociate, forming phenolate anions, while the surface functional groups are negatively charged. The electrostatic repulsion between the identical charges lowers the adsorption capacities, between the negative surface charge and the phenolate anions and between phenolate–phenolate anions in the solutions (Hameed et al., 2008). On the other hand, there might be a competition between the OH^- ions and the ionic species of BPA or TCP, hence reducing BPA and TCP removal amount. Besides, the phenolate anions have higher solubility in aqueous solution and form stronger adsorbate–water bonds, so the adsorption is more difficult at higher pH. Despite these factors, significant removal was observed at alkaline pH, especially for BPA (83% at pH 10), which indicates that physisorption rather than chemisorption might be involved in the removal process (Djebri et al., 2016, 2017). Fig. 5 shows that the initial solution pH has much greater influence on TCP removal than that in the case of BPA, which could be attributed to the acidic character of the solute molecules. BPA and TCP are weak acids (pK_a values 9.6 and 6.8, respectively, at ambient temperature). The lower pK_a value is associated with the electron withdrawal effect of the substitution on the aromatic ring, thus reducing the overall electron density of aromatic ring of the adsorbate (Laszlo et al., 2004). Similar results have been reported by various researchers on the adsorption of chlorophenols by activated carbon (Ren et al., 2011; Hameed et al., 2008; Laszlo and Szucs, 2001).

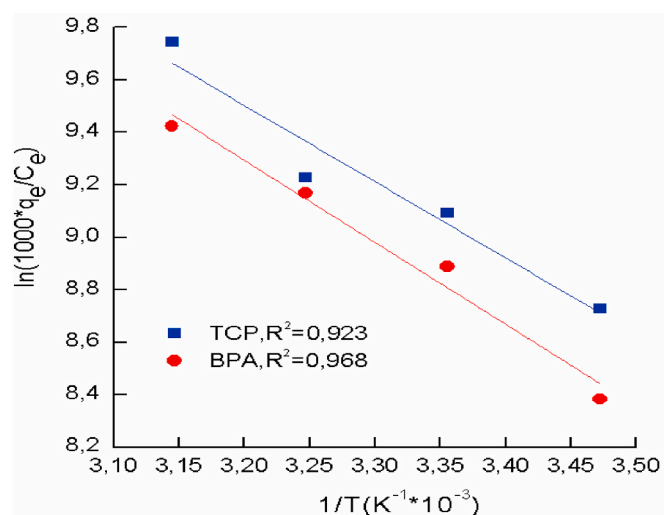


Fig. 6. Effect of temperature on adsorption of BPA and TCP onto A-AC composite.

Table 5

Thermodynamic parameters for the adsorption of TCP and BPA onto A-AC composite.

EDCs	T(K)	ΔG° (kJ/mol)	ΔH° (kJ/mol)	ΔS° (J/mol K)
TCP	288	−20.86	24.18	156.40
	298	−22.42		
	308	−23.99		
	318	−25.55		
BPA	288	−20.21	26.01	160.49
	298	−21.82		
	308	−23.42		
	318	−25.03		

3.4. Effect of temperature on adsorption and thermodynamic studies

The effect of temperature of the BPA and TCP adsorption on the A-AC was investigated under isothermal conditions in the temperature range 15–45 °C. The BPA and TCP adsorption capacity onto A-AC increase with increasing temperature, suggesting that the adsorption reaction is endothermic. The thermodynamic parameters were estimated to evaluate the feasibility and the nature of the adsorption process. Gibbs' free energy (ΔG° , kJ/mol), enthalpy (ΔH° , kJ/mol) and entropy (ΔS° , J/mol. K) changes were calculated at various temperatures (288, 298, 308 and 318 K) to predict the nature of adsorption and were estimated using below equations (Djebri et al., 2016):

$$\Delta G = -RT \ln K \quad (15)$$

$$\log \left(\frac{1000 \times q_e}{C_e} \right) = \frac{\Delta S^\circ}{2.303R} - \frac{\Delta H^\circ}{2.303RT} \quad (16)$$

where q_e is the adsorbed amount of BPA or TCP per unit of mass of A-AC (mg/g), C_e is equilibrium concentration (mg/L), R is the universal gas constant (8.314 J/mol. K); T , is temperature in Kelvin (K). And from the plot of $\log (1000 \times q_e/C_e)$ vs. $1/T$ (R^2 : 0.97 and 0.92 for BPA and TCP, respectively) (Fig. 6.), the intercept and slope were used to determine the values of ΔH° and ΔS° , respectively (Table 5). The values of ΔG° are negative, indicating the feasibility of the process and suggesting that the adsorption of BPA and TCP onto A-AC is a spontaneous and physical process. The positive values of ΔH° (24.2 kJ/mol and 26.0 kJ/mol for BPA and TCP, respectively) indicate that the adsorption process is endothermic in nature. The positive values of ΔS° suggest that the degree of freedom increases at the solid-liquid interface during the adsorption of TCP and BPA.

Table 6

Comparison of maximum monolayer adsorption capacity on various adsorbents reported in literature.

Adsorbate	Adsorbent	C_i (mg. L^{-1})	q_m (mg. g^{-1})	Reference
BPA	Calcium alginate/organo activated bentonite (A-OAB)	30–300	252.9	This study
	Calcium alginate/activated carbon (A-AC)	30–300	419.0	This study
	Calcium alginate/activated carbon (A-AC)	20–700	368.3	This study (Djebri et al., 2017)
	Calcium alginate/organo-activated bentonite/activated carbon (A-AC-OAB)	1–30	127.7	(2017)
	Organobentonite	7–55	28.1	Zhou et al. (2016)
	Fe ₃ O ₄ -polyaniline	20–600	181.2	(2016)
	Rice straw	25–500	263.1	Chang et al. (2012)
	Commercial activated carbon		382.1	Bautista-Toledo et al. (2005)
	Commercial activated carbon			Liu et al. (2009)
	Calcium alginate/organo activated bentonite (A-OAB)	15–400	336.7	This study
	Calcium alginate/activated carbon (A-AC)	15–400	444.8	This study
	Calcium alginate/organo-activated bentonite/activated carbon (A-AC-OAB)	15–400	385.0	This study (Djebri et al., 2017)
	Organobentonite	20–800	244.6	(2017)
	Cattail fiber-activated carbon	25–500	192.3	Ren et al. (2011)
TCP	Magnetic molecularly imprinted Fe ₃ O ₄ carbon nanospheres	25–500	200	Wang et al. (2015)
	β -cyclodextrinmesoporous attapulgite composites	2–400	65.2	Zheng et al. (2016)

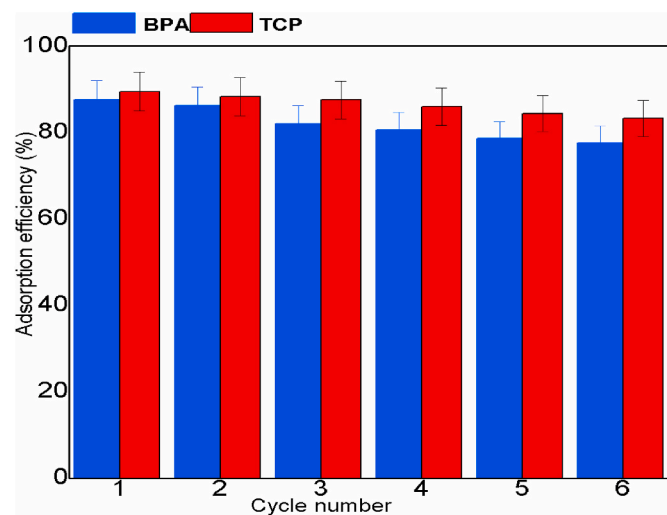


Fig. 7. The results of regeneration test for the adsorption of BPA and TCP onto A-AC.

3.5. Comparison of adsorption of BPA and TCP on various adsorbents

Table 6, lists the maximum monolayer adsorption capacity of TCP and BPA on various adsorbents. The high adsorption capacity of A-AC found in this study reveals that this composite is a promising adsorbent for TCP and BPA removal.

3.6. Adsorbent regeneration

Very few studies on adsorbent materials have been complemented by

experiments on pollutant desorption. When the adsorption equilibrium is reached, the adsorbent cannot adsorb the target adsorbate anymore. A regeneration step is an important process used to restore the adsorption capacity. The viability of regenerating the exhausted A-AC saturated with both TCP and BPA was evaluated using ethanol desorption technique. The results of the regeneration studies are graphically presented in Fig. 7. This figure shows BPA and TCP adsorption removal (%) for six cycles of successive adsorption/desorption cycles. Adsorption was performed at pH close to 7 and 4 for BPA and TCP, respectively. It can be observed that the amount of desorbed BPA or TCP was quite high and that the adsorbed amount of BPA or TCP remained almost the same, even after six cycles. Nevertheless, as seen from Fig. 7, the total adsorption capacities of both BPA and TCP slightly decreased after six-time regenerations (11 and 7% for BPA and TCP, respectively). This small drop in the adsorption capacities could be ascribed to the fact that the regeneration process might result in the decrease of binding sites (Zheng et al., 2016; Zhou et al., 2012). Furthermore, regeneration experiments confirm the good stability of A-AC after multicycle tests.

3.7. Characterization of A-AC composite adsorbent

SEM images were taken at 50 x (Fig. 8a) 150 x (Figs. 8b) and 25 x (Fig. 8c) magnifications, as shown in Fig. 8. The surface of activated carbon AC (Fig. 8a) is characterized by grooves, irregular ridges, channels and bright spots, which appeared undulated due to the presence of intermittently spaced protrusions (Jawad et al., 2016; Şimşek, 2016). The distribution of pore sizes is irregular with a variable holes size, which implied a wide surface area for active sites for adsorption. The alginate beads A (Fig. 8b) have a smooth surface with streaks. The structure is homogeneous with a regular surface porosity and a relatively uniform morphology. In the case of A-AC beads (Fig. 8c), sphericity is confirmed; their surface is relatively smooth and has undulations. These beads exhibit a bright and clear morphology with a heterogeneous (Jodraet and Mijangos, 2003; Saavedra-Labastida et al., 2019).

FTIR spectra of A-AC before and after adsorption of BPA and TCP are depicted in Fig. 9. The broad absorption band at 3300–3600 cm^{-1} with a maximum at about 3424 cm^{-1} is characteristic of the stretching vibration of hydrogen-bonded hydroxyl groups (from carboxyls, phenols or alcohols) and adsorbed water onto A-AC (Feng et al., 2011). The ν (C–H) stretching bands are detectable at 2922 and 2855 cm^{-1} . The strong asymmetric and weak symmetric stretching vibration bands of –COO observed at 1615 and 1415 cm^{-1} are caused by the alginate molecules (Suarez et al., 2009; Hassan et al., 2014a). The band at 800 cm^{-1} is attributed to out of-plane deformation mode of C–H for different substituted benzene rings. After the adsorption of BPA and TCP onto A-AC, many functional groups shifted to different bands. The bands at 3424, 1615, 1080 and 800 cm^{-1} transferred to higher frequencies at 3481, 1635, 1111 and 806 for TCP and 3441, 1633, 1097 and 811 for BPA, respectively. Whereas the peak at 1415 cm^{-1} shifted slightly to a lower frequency band at 1409 and 1413 cm^{-1} , for BPA and TCP, respectively. On the contrary, the peaks at 630 and 476 cm^{-1} appeared after adsorption. These changes indicated the possible interaction of surface sites of A-AC with BPA and TCP (Rosal et al., 2010).

For better understanding of adsorption mechanism, the pH_{PZC} of A and AC (figure not shown) were determined and found to be 6.6 and 3.0, respectively; while the pH_{PZC} of A-AC was found to be 4.5 (See Fig. 5. Inset), indicating the acid character of A-AC surface, which is in agreement with the presence of acid groups appeared in the FTIR spectrum. Below the pH_{PZC} value, the surface of A-AC is positively charged, favoring the adsorption of anions via electrostatic forces attractions. Above the pH_{PZC} , the surface has a negative charge, which favors the adsorption of cation species.

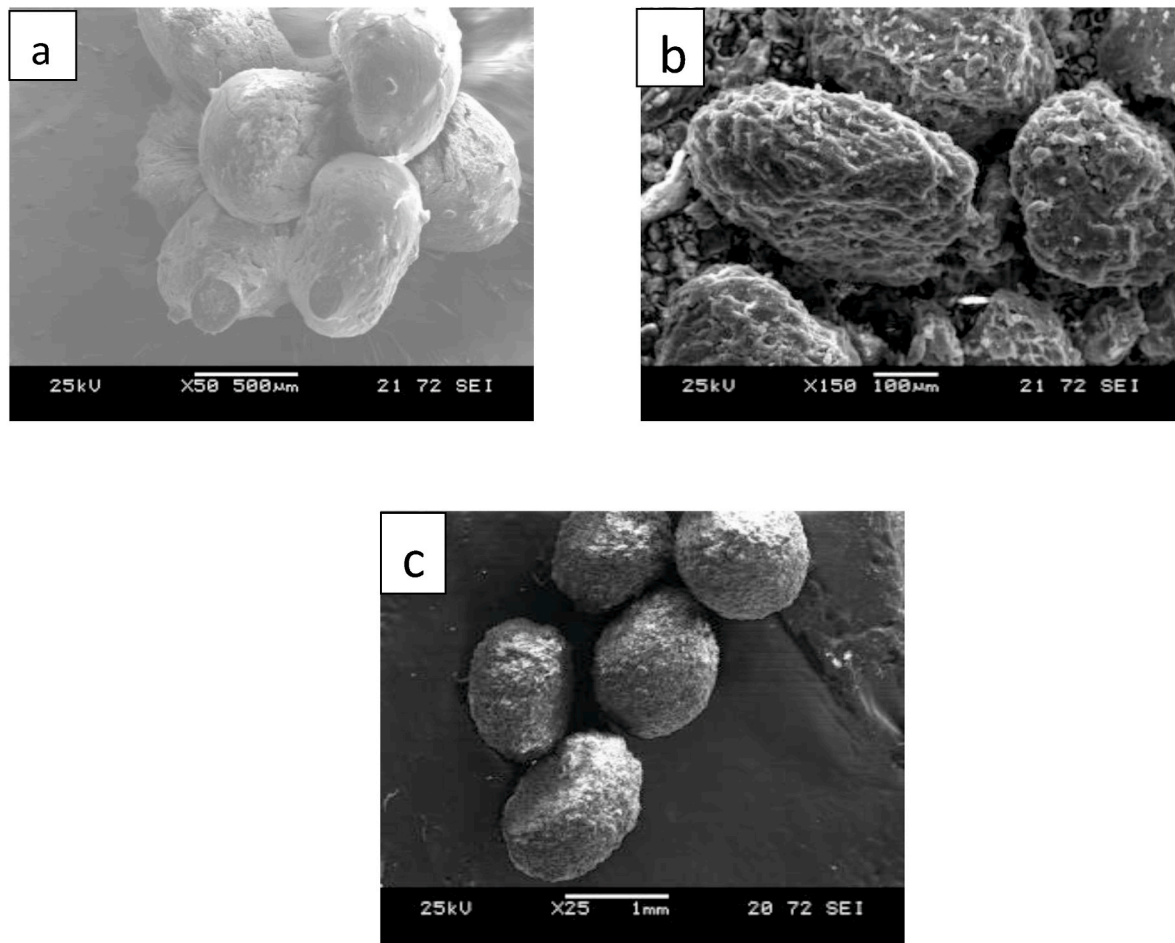


Fig. 8. SEM images of the (a) A, (b) AC and (c) A-AC samples.

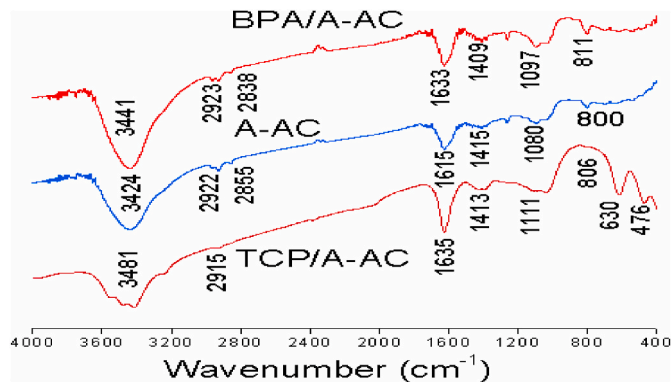


Fig. 9. FTIR patterns of A-AC before and after adsorption of BPA and TCP.

4. Conclusion

In the present paper A-OAB, A-AC and A-AC-OAB were prepared and used in the removal of BPA and TCP from wastewater. A-AC is the most efficient adsorbent among the tested adsorbents considering its high and fast adsorption capacity and the following results were obtained: (1) the adsorption of BPA and/or TCP from aqueous solutions was shown that the pseudo-second-order kinetic fits well with the experimental data. (2) The equilibrium adsorption data are well fitted to both Langmuir and Freundlich models and the monolayer saturation capacity was found at 25 °C to be 419 and 444 mg/g for BPA and TCP onto A-AC, respectively. (3) It was also determined to be feasible, especially in an acidic medium,

yet it decreased as pH increased due to a simultaneous change in surface charges and partial solute ionization. (4) The obtained data from the adsorption-desorption experiments illustrate efficient and stabilized performance of A-AC during repeated cycles. The present study concludes that the A-AC composite material based on alginate and activated carbon significantly enhances the removal of emerging compounds from aqueous solutions and showing excellent regeneration capacity, may be used as an efficient material and alternative to more costly adsorbents for the removal of pollutants from wastewater.

Declaration of competing interest

The authors declare that they have no known competing financial interests or personal relationships that could have appeared to influence the work reported in this paper.

References

- Achak, M., Hafidi, A., Ouazzani, N., Sayadi, S., Mandi, L., 2009. Low cost biosorbent "banana peel" for the removal of phenolic compounds from olive mill wastewater: kinetic and equilibrium studies. *J. Hazard Mater.* 166, 117–125.
- Ahmaruzzaman, M., Reza, R.A., 2015. Decontamination of cationic and anionic dyes in single and binary mode from aqueous phase by mesoporous pulp waste. *Environ. Prog. Sustain. Energy* 34, 724–735.
- Bautista-Toledo, I., Ferro-García, M., Rivera-Utrilla, J., Moreno Castilla, C., Fernández, F., 2005. Bisphenol A removal from water by activated carbon. Effects of carbon characteristics and solution chemistry. *Environ. Sci. Technol.* 39 (16), 6246–6250.
- Belhouchat, N., Zaghouane-Boudiaf, H., Viseras, C., 2017. Removal of anionic and cationic dyes from aqueous solution with activated organo-bentonite/sodium alginate encapsulated beads. *Appl. Clay Sci.* 135, 9–15.

- Bolong, N., Ismail, A.F., Salim, M.R., Matsuura, T.A., 2009. Review of the effects of emerging contaminants in wastewater and options for their removal. *Desalination* 239, 229–246.
- Boukhalfa, N., Boutahala, M., Djebri, N., 2016. Synthesis and characterization of ZnAl-layered double hydroxide and organo-K10 montmorillonite for the removal of diclofenac from aqueous solution. *Adsorpt. Sci. Technol.* 1–17, 0(0).
- Chang, K.-L., Hsieh, J.-F., Ou, B.-M., Chang, M.-H., Hsieh, W.-Y., Lin, J.-H., Huang, P.-J., Wong, K.-F., Chen, S.-T., 2012. Adsorption studies on the removal of an endocrine-disrupting compound (bisphenol A) using activated carbon from rice straw. *Agricultural Waste Sep Sci Technol* 47, 1514–1521.
- Deblonde, T., Cossu-Leguille, C., Hartemann, P., 2011. Emerging pollutants in wastewater: a review of the literature. *Int. J. Hyg Environ. Health* 214, 442–448.
- Djebri, N., Boutahala, M., Chelali, N., Boukhalfa, N., Zeroual, L., 2016. Enhanced removal of cationic dye by calcium alginate/organobentonite beads: modeling, kinetics, equilibria, thermodynamic and reusability studies. *Int. J. Biol. Macromol.* 92, 1277–1287.
- Djebri, N., Boutahala, M., Chelali, N., Boukhalfa, N., Larbi, Z., 2017. Adsorption of bisphenol A and 2,4,5-trichlorophenol onto organo-acid-activated bentonite from aqueous solutions in single and binary systems. *Desal. Wat. Treat* 1–11.
- El Fargani, H., Lakhmiri, R., El Farissi, H., Albourine, A., Safi, M., Cherkaoui, O., 2017. Removal of anionic dyes by silica-chitosan composite in single and binary systems: valorization of shrimp co-product “Crangon-Crangon” and “Pandalus Borealis”. *J. Mater. Environ. Sci.* 8, 724–739.
- Feng, N., Guo, X., Liang, S., Zhu, Y., Liu, J., 2011. Biosorption of heavy metals from aqueous solutions by chemically modified orange peel. *J. Hazard Mater.* 185, 49–54.
- Gholizadeh, A., Kerami, M., Gholami, M., Farzadki, M., 2013. Kinetic and isotherm studies of adsorption and biosorption processes in the removal of phenolic compounds from aqueous solutions: comparative study. *J Environ Health SciEng* 11–29.
- Gupta, V.K., Carrott, P.J.M., Ribeiro Carrott, M.M.L., Suhas, T.L., 2009. Low-cost adsorbents: growing approach to wastewater treatment—a review. *Crit. Rev. Environ. Sci. Technol.* 39, 783–842.
- Hameed, B.H., Tan, I.A.W., Ahmad, A.L., 2008. Adsorption isotherm, kinetic modeling and mechanism of 2,4,6-trichlorophenol on coconut husk-based activated carbon. *Chem. Eng. J.* 144, 235–244.
- Hassan, A.F., Abdel-Mohsen, A.M., Fouda, Moustafa M.G., 2014a. Comparative study of calcium alginate, activated carbon, and their composite beads on methylene blue adsorption. *Carbohydr. Polym.* 102, 192–198.
- Hassan, A.F., Abdel-Mohsen, A.M., Elhadidy, H., 2014b. Adsorption of arsenic by activated carbon, calcium alginate and their composite beads. *Int. J. Biol. Macromol.* 68, 125–130.
- Jawad, A.H., Rashid, R.A., MohdIshak, M.A., Wilson, D.L., 2016. Adsorption of methylene blue onto activated carbon developed from biomass waste by H₂SO₄ activation: kinetic, equilibrium and thermodynamic studies. *Desal. Wat. Treat.* 1–13.
- Jodraet, Y., Mijangos, F., 2003. Phenol adsorption in immobilized activated carbon with alginate gels. *Sep Sci Technol* 38 (8), 1851–1867.
- Laszlo, K., Szucs, A., 2001. Surface characterization of polyethyleneterephthalate (PET) based activated carbon and the effect of pH on its adsorption capacity from aqueous phenol and 2,3,4-trichlorophenol solutions. *Carbon* 39, 1945–1953.
- Laszlo, K., Tombacz, E., Kerepesi, P., 2004. Surface chemistry of nanoporous carbon and effect of pH on adsorption from aqueous phenol and 2,3,4-trichlorophenol solutions. *Colloid. Surface. Physicochem. Eng. Aspect.* 230, 13–22.
- Liu, G., Ma, J., Li, X., Qin, Q., 2009. Adsorption of bisphenol A from aqueous solution onto activated carbons with different modification treatments. *J. Hazard Mater.* 164, 1275–1280.
- Luo, W., Huang, Q., Antwi, P., Guo, B., Sasaki, K., 2020. Synergistic effect of ClO⁴⁻ and Sr²⁺ adsorption on alginate-encapsulated organo-montmorillonite beads: implication for radionuclide immobilization. *J. Colloid Interface Sci.* 560, 338–348.
- Mavinkattimath, R.G., Kodialbail, V.S., 2017. Simultaneous adsorption of Remazol brilliant blue and Disperse orange dyes on red mud and isotherms for the mixed dye system. *Environ. Sci. Pollut. Res.* 24, 18912–18925, 59.
- Pham, T.T., Proulx, S., 1997. PCBs and PAHs in the montreal urban community (quebec, Canada) wastewater treatment plant and in the effluent plume in the St Lawrence river. *Water Res.* 31 (8), 1887–1896.
- Ren, L., Zhang, J., Li, Y., Zhang, C., 2011. Preparation and evaluation of cattail fiber based activated carbon for 2,4-dichlorophenol and 2,4,6-trichlorophenol removal. *Chem. Eng. J.* 168, 553–561.
- Rosal, R., Rodriguez, A., Perdigon-Melon, J.A., Petre, A., Garcia-Calvo, E., Gomez, M.J., Aguerre, A., Fernandez-Alba, A.R., 2010. Occurrence of emerging pollutants in urban wastewater and their removal through biological treatment followed by ozonation. *Water Res.* 44, 578–588.
- Rossner, A., Snyder, S.A., Knappe, D.R.U., 2009. Removal of emerging contaminants of concern by alternative adsorbents. *Water Res.* 43, 3787–3796.
- Saavedra-Labastida, E., Díaz-Nava, M.C., Illescas, J., 2019. Comparison of the removal of an anionic dye from aqueous solutions by adsorption with organically modified clays and their composites. *Water Air Soil Pollut.* 230, 88. <https://doi.org/10.1007/s11270-019-4131-z>.
- Sathishkumar, M., Binupriya, A.R., Kavitha, D., Yun, S.E., 2007. Kinetic and isothermal studies on liquid-phase adsorption of 2, 4-dichlorophenol by palm pith carbon. *Bioresour. Technol.* 98, 866–873.
- Sdiri, A.T., Higashi, T., Jamoussi, F., 2014. Adsorption of copper and zinc onto natural clay in single and binary systems. *Int. J. Environ. Sci. Technol.* 11, 1081–1092.
- Shaarani, F.W., Hameed, B.H., 2010. Batch adsorption of 2,4-dichlorophenol onto activated carbon derived from agricultural waste. *Desalination* 255, 159–164.
- Şimşek, S., 2016. Adsorption properties of lignin containing bentonite–polyacrylamide composite for ions. *Desal. Water Treat.* 57, 23790–23799.
- Suarez, S., Lema, J.M., Omil, F., 2009. Pre-treatment of hospital wastewater by coagulation–flocculation and flotation. *Bioresour. Technol.* 100, 2138–2146.
- Sun, Y., Yue, Q., Gao, B., Huang, L., Xu, X., Li, Q., 2012. Comparative study on characterization and adsorption properties of activated carbons with H₃PO₄ and H₄P₂O₇ activation employing *Cyperus alternifolius* as precursor. *Chem. Eng. J.* 181–182, 790–797.
- Tan, I.A.W., Ahmad, A.L., Hameed, B.H., 2009. Adsorption isotherms, kinetics, thermodynamics and desorption studies of 2,4,6-trichlorophenol on oil palm empty fruit bunch-based activated carbon. *J. Hazard Mater.* 164, 473–482.
- Tong, D.S., Zhou, C.H., Lu, Y., Yu, H., Zhang, G.F., Yu, W.H., 2010. Adsorption of acid red G dye on octadecyltrimethylammonium montmorillonite. *Appl. Clay Sci.* 50, 427–431.
- Vogelsang, C., Grung, M., Jantsch, T.G., Tollefsen, K.E., Liltved, H., 2006. Occurrence and removal of selected organic micropollutants at mechanical, chemical and advanced wastewater treatment plants in Norway. *Water Res.* 40, 3559–3570.
- Wang, J., Pan, J., Yin, Y., Wu, R., Dai, X., Dai, J., Gao, L., Ou, H., 2015. Thermo-responsive and magnetic molecularly imprinted Fe₃O₄@ carbon nanospheres for selective adsorption and controlled release of 2, 4, 5-trichlorophenol. *J. Ind. Eng. Chem.* 25, 321–328.
- Zheng, X., Dai, J., Pan, J., 2016. Synthesis of β-cyclodextrin/mesoporous attapulgite composites and their novel application in adsorption of 2,4,6-trichlorophenol and 2,4,5-trichlorophenol. *Desal. Water Treat.* 57, 14241–14250.
- Zhou, Y., Lu, P., Lu, J., 2012. Application of natural biosorbent and modified peat for bisphenol A removal from aqueous solutions. *Carbohydr. Polym.* 88, 502–508.
- Zhou, Q., Wang, Y., Xiao, J., Fan, H., 2016. Adsorption and removal of bisphenol A, α-naphthol and β-naphthol from aqueous solution by Fe₃O₄@polyaniline core-shell nanomaterials. *Synth. Met.* 212, 113–122.